

# OVERALL PERFORMANCE COMPARISON OF S-BAND C-BAND, AND X-BAND BASED COMPACT XFEL FACILITIES

Yujong Kim<sup>1,2,3,\*</sup>, S. Setiniyaz<sup>1</sup>, M. Titberidze<sup>1</sup>, and K. H. Jang<sup>4</sup>

<sup>1</sup>Department of Physics, Idaho State University, Pocatello, ID 83209, USA

<sup>2</sup>Idaho Accelerator Center, Idaho State University, Pocatello, ID 83201, USA

<sup>3</sup>Thomas Jefferson National Accelerator Facility, Newport News, VA 23606, USA

<sup>4</sup>Korea Atomic Energy Research Institute, Daejeon 305-353, Korea

## Abstract

Recently, there were several activities to build much more compact XFEL facilities, which are based on C-band and X-band RF linac technologies. But up to now, there was no detailed research to compare the performance of S-band, C-band, and X-band RF linac based compact XFEL facilities. To compare the performance, recently, Idaho State University Next-generation advanced Accelerators & ultrafast Beams Lab (ISU NABL) members have designed three different XFEL facilities where the S-band, C-band, and X-band RF linac technologies are used for the main FEL driving linacs. In this paper, we describe layouts, start-to-end simulations, and comparison of overall performance of those three XFEL facilities. In addition, we also describe control of energy chirp, RF jitter tolerances, alignment and transverse wakefield issue, and bandwidth of XFEL photon beam in C-band or X-band based compact XFEL facilities.

## INTRODUCTION

Recently, several leading national laboratories around world have constructed or plans to construct new XFEL facilities. Among them, SPring-8 Angstrom Compact free electron LASER (SACLA) of SPring-8 in Japan was constructed by using the C-band RF linac technology due to the limitation in available site for their XFEL facility [1]. After considering the performance of the XFEL driving linac and an available site for the facility, similarly, PSI in Switzerland also determined to build their SwissFEL facility with the same C-band RF linac technology [2]. After the successful XFEL lasing at SACLA, demand on compact XFEL facilities becomes much stronger. Recently, there were several activities to build much more compact XFEL facilities with a higher RF frequency. However, there are merits and demerits when we use a higher RF frequency for the XFEL driving main linac. To compare overall performance of the various XFEL driving linacs, ISU NABL members have designed three different XFEL facilities where the S-band, C-band, and X-band RF linac technologies are used in the XFEL driving main linacs after the second bunch compressor (BC2). Here, to supply the same initial beam conditions up to BC2, a common S-band injector and linac from the gun cathode to BC2 are used in three different XFEL facilities. In this paper, we describe how to control the en-

ergy chirp and energy spread at the end of the XFEL driving linac, and compare overall performance of those three XFEL facilities, where RF jitter tolerances, alignment and transverse short-range wakefield issue, and bandwidth of XFEL photon beam are discussed.

## ENERGY CHIRP VS. XFEL BANDWIDTH

Generally, the bandwidth of XFEL photon beams becomes wider, and the brilliance of XFEL photon beams is also dropped if the projected energy spread of the electron bunch is larger at the entrance of undulators where the XFEL photon beams are generated [3]. That means that the energy chirp in the longitudinal phase space of the electron beam should be flat or minimized to obtain the minimum projected energy spread and to get the narrowest bandwidth and the highest brilliance of the XFEL photon beams [3].

For a Gaussian electron beam, the rms relative projected energy spread  $\sigma_\delta$  after an RF linac is a function of the longitudinal short-range wakefield  $W_{||}$ , single bunch charge  $Q = Ne$ , rms bunch length  $\sigma_z$ , RF frequency  $f_{rf} = \kappa_{rf}c/2\pi$ , RF gradient  $G$ , and RF phase  $\phi_{rf}$  of the linac, and it is given by

$$\sigma_\delta \simeq \left| \frac{(1 + 0.25i)3.04\pi\epsilon_0 N r_e W_{||} (1.3\sigma_z)}{2.35G \cos \phi_{rf}} - \sigma_z \kappa_{rf} \tan \phi_{rf} \right|, \quad (1)$$

where  $\epsilon_0$  is the permittivity of free space,  $N$  is the number of electrons per bunch,  $e$  is the single electron charge,  $\kappa_{rf}$  is the wave number of the RF linac, and  $c$  is the speed of light [3, 4]. Since the longitudinal short-range wakefield  $W_{||}$  of a long periodic linac structure is a function of the average iris radius  $a$  and the periodic cell length  $L$  in the linac structure, the rms relative projected energy spread  $\sigma_\delta$  also depends on them, and the minimum  $\sigma_\delta$  can be obtained when the real part of Eq. (1) is zero [3–5]. Therefore, the minimum projected energy spread and minimum XFEL bandwidth can always be obtainable by choosing a proper RF gradient  $G$  and a proper phase  $\phi_{rf}$  of the linac for a given linac structure, a given bunch length, and a given bunch charge [3].

As summarized in Table 1 and as shown in Fig. 1, average geometric parameters  $a$ ,  $b$ ,  $g$ , and  $L$  of common European S-band, C-band, and X-band linac structures are

\* E-Mail: yjkim@ISU.edu

Table 1: Average Parameters of Linac Structures [3]

Parameter	Unit	S-band	C-band	X-band
RF frequency	MHz	2998	5996	11992
iris radius $a$	mm	11.003	6.954	4.548
outer radius $b$	mm	40.151	20.101	10.713
cell gap $g$	mm	28.333	14.167	8.714
cell period $L$	mm	33.333	16.667	10.410

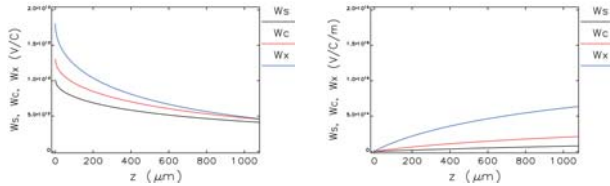


Figure 1: Longitudinal short-range wakefields (left) and transverse short-range wakefields (right) of S-band (black), C-band (red), and X-band (blue) linac structures as summarized in Table 1. Here  $z$  means the longitudinal distance between one wake-receiving electron and the other wake-generating electron in a bunch [3].

investigated, and their longitudinal and transverse short-range wakefields are plotted to compare their magnitudes and nonlinearity [3, 5]. Since the rms bunch length after BC2 in the XFEL driving linac is generally shorter than  $15 \mu\text{m}$ , which corresponds to about  $90 \mu\text{m}$  in the full width, the transverse short-range wakefield of the C-band linac structure is similar to that of the S-band linac structure for such a short bunch,  $z \leq 90 \mu\text{m}$  as shown in Fig. 1. However, the transverse short-range wakefield of the X-band linac structure is somewhat bigger than those of S-band and C-band linacs. In addition, the longitudinal short-range wakefield of the X-band linac structure is much stronger and nonlinear than those of the S-band and C-band linac structures for such a short bunch length as shown in Fig. 1.

As shown in Figs. 2 and 3(bottom), the initial large energy chirp and the initial big rms relative projected energy spread of  $\sigma_\delta = 0.473\%$  after BC2 can be damped down by the action of the longitudinal short-range wakefield in a 205.14 m long X-band linac [3]. By optimizing the RF gradient and RF phase of the linac properly, the initial big energy spread can be damped down to about 0.02% as shown in Figs. 2(top-left), 2(middle-right), and 2(bottom-right). Here, electron beam is accelerated from 1.469 GeV to about 6.0 GeV by the X-band linac, and all initial beam parameters at the entrance of the X-band linac are same for all five cases in Fig. 2, but only RF gradient and RF phase are different for those cases. Figures. 2(top-right), 2(middle-left), and 2(middle-right) show the impact of the RF phase on the energy chirp and the rms energy spread for an RF gradient of 40 MV/m, and Figs. 2(middle-left), 2(bottom-left), and 2(bottom-right) show the impact of the RF gradient on the energy chirp and the rms energy spread for an RF phase of -5 degree [3].

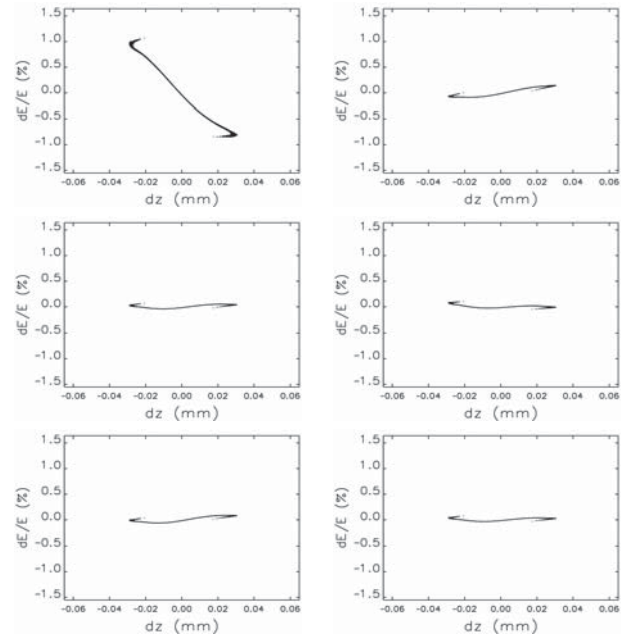


Figure 2: Longitudinal phase spaces showing compensation of the energy chirp and damping of the projected energy spread after a 205.14 m long X-band linac: (top-left) the initial phase space at the entrance of the X-band linac with  $\sigma_\delta = 0.473\%$ , (top-right) the final phase space at the exit of the linac with  $\sigma_\delta = 0.074\%$  for an RF gradient of 40 MV/m and an RF phase of +5 degree, (middle-left) the final phase space with  $\sigma_\delta = 0.032\%$  for 40 MV/m and -5 degree, (middle-right) the final phase space with  $\sigma_\delta = 0.022\%$  for 40 MV/m and -10 degree, (bottom-left) the final phase space with  $\sigma_\delta = 0.051\%$  for 36 MV/m and -5 degree, and (bottom-right) the final phase space with  $\sigma_\delta = 0.024\%$  for 44 MV/m and -5 degree [3].

## OPTIMIZED XFEL LINACS

As shown in Fig. 3, three S-band, C-band, and X-band RF linac technology based 6.0 GeV XFEL facilities are designed to generate XFEL photon beam at 0.1 nm with a 50 m long in-vacuum undulator [2, 3]. To compare performance of XFEL driving main linacs after BC2 properly, all initial beam parameters right after BC2 should be same for those three XFEL linacs. Therefore, a common S-band injector and linac from the gun cathode to BC2 are used as shown in Fig. 3. To optimize the RF gradient, RF phase, and RF distributions of the main linac after BC2, we have considered possible RF power sources, SLED gain, length of linac structures, FODO cell length, available tunnel length, total linac length, compensation of the final energy chirp and the minimum energy spread after the main linac, and RF jitter tolerance. Specially, all linacs were optimized to have the flat energy chirp or the minimum energy spread at the entrance of the undulator. In addition, to reduce RF phase jitter, the RF phases were optimized to have the near-on-crest RF phases for C-band and X-band RF linacs. Their detailed layouts of the RF dis-

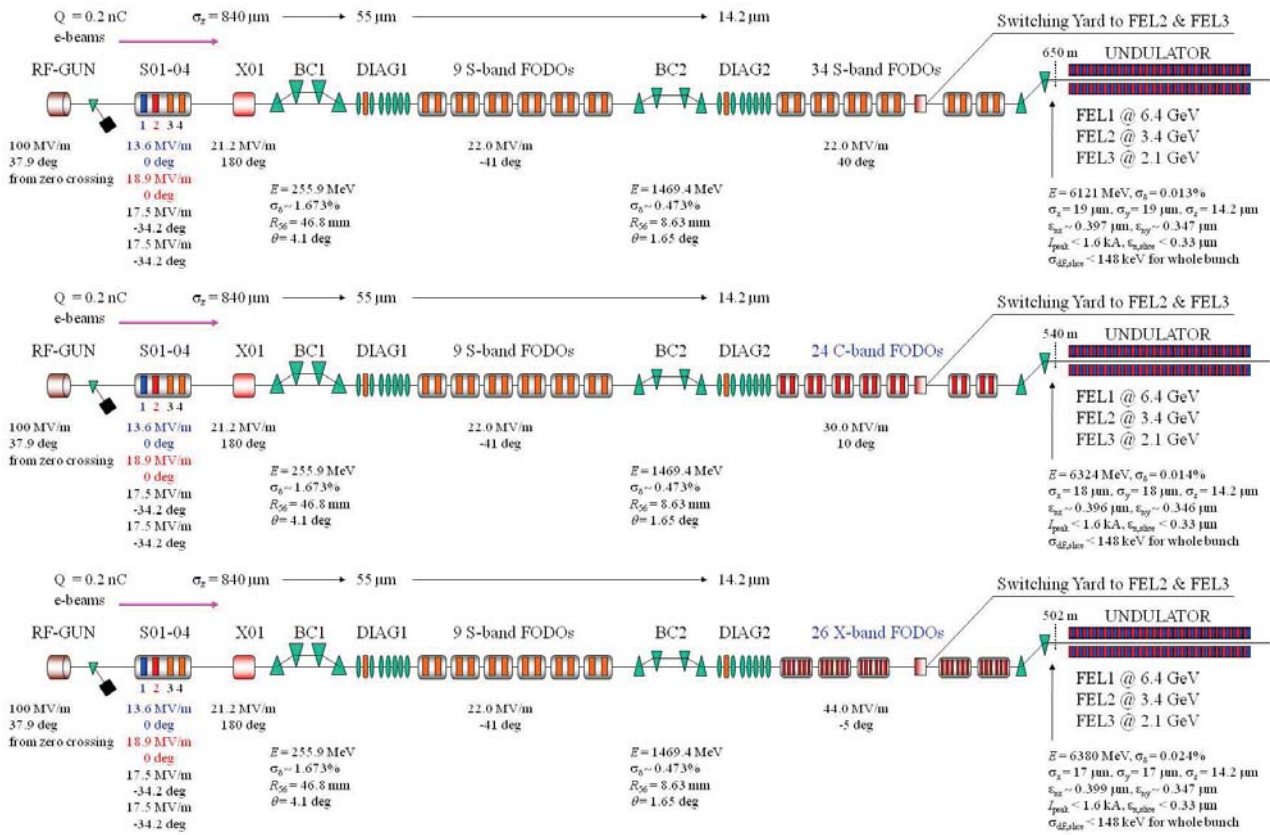


Figure 3: Layouts of S-band (top), C-band (middle), and X-band (bottom) based XFEL driving linacs [3].

tribution systems and linac FODO lattices can be found in a reference [3]. The key parameters of those three optimized linacs are summarized in Table 2, and the peak current and slice emittances and slice energy spread of the S-band based XFEL facility are shown in Fig. 4. Please note that the peak current and slice parameters of the C-band and X-band based XFEL facilities are close to those of S-band based XFEL facility [3]. Therefore, there is no big difference between those three linac facilities if we look into only slice parameters and peak current. However, there are some differences if we look into the nonlinearity in the longitudinal phase space, the energy chirp, the projected energy spread, the FEL photon beam bandwidth, total linac length, sensitivities on RF jitters and misalignments, and construction budget as summarized in Table 2.

In case of the S-band linac based XFEL facility, originally, we chose 0 degree for the RF phase of the S-band main linac after BC2 to get the maximum energy gain in the linac, to reduce the linac length, and to reduce the sensitivity of the RF phase errors. However, as shown in Fig. 5(top-left), in this case, the energy chirp was not compensated effectively, and the rms relative projected energy spread was about 0.068% due to the weak longitudinal short-range wakefield of the S-band linac. As shown in Fig. 5(top-right), we can obtain the best energy chirp and the minimum energy spread of 0.013% by changing its RF phase from 0 degree to 40 degree for a given RF gradient

Table 2: Key Parameters of Three Optimized Linacs [3]

Parameter	Unit	S-band	C-band	X-band
final beam energy	GeV	6.121	6.324	6.380
normalized rms emittance	$\mu\text{m}$	0.397	0.396	0.399
peak current at core	kA	1.6	1.6	1.6
slice emittance at core	$\mu\text{m}$	0.33	0.33	0.33
rms slice energy spread	keV	148	148	148
RF gradient of linac	MV/m	22	30	44
RF phase of linac	deg	40	10	-5
no of linac structure	.	68	96	156
no of 100 MW modulator	.	34	48	26
structures per modulator	.	2	2	6
no of klystron	.	34	48	26
no of FODO cells	.	34	24	26
length of a FODO cell	m	10.4	9.9	7.89
length of linac after BC2	m	353.6	237.6	205.14
RF power of klystron	MW	45	50	50
SLED gain with a margin	.	2.5	2.63	4.8
power margin	%	15	24	10
impact of RF jitter	.	middle	low	high
impact of misalignment	.	low	low	middle
nonlinearity in long. phase	.	weak	weak	strong
rms energy spread $\sigma_\delta$	%	0.013	0.014	0.024
rms FEL bandwidth $\Delta\lambda/\lambda$	%	0.05	0.05	0.10

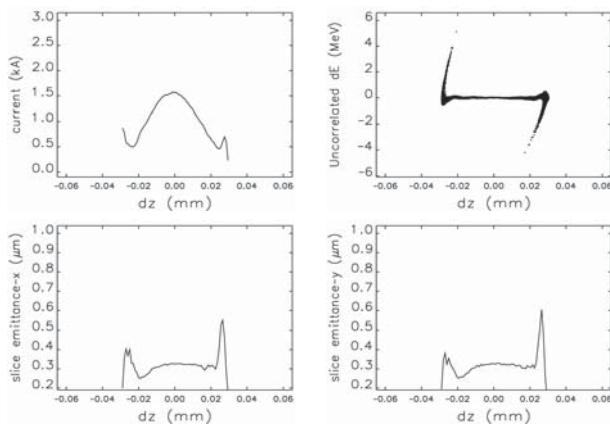


Figure 4: Peak current and slice parameters at the end of S-band based XFEL linac [3].

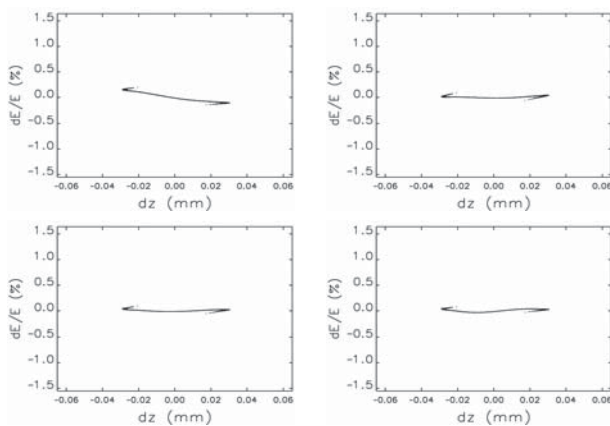


Figure 5: Longitudinal phase spaces at the end of S-band (top-left and top-right), C-band (bottom-left) and, X-band (bottom-right) based XFEL linacs [3].

of 22 MV/m. Therefore, the sensitivity of the RF phase errors becomes worse even though we could get a better FEL photon beam bandwidth with 40 degree. To solve this RF phase error issue and to use a near on-crest RF phase, a linac with a much higher RF gradient or a much longer linac is required. But there is limitation for us to choose a much longer linac for the compact XFEL facility and we can't choose a much higher RF gradient with the S-band RF linac technology either.

These difficulties can be easily solved by using compact C-band and X-band RF linacs, which can supply higher gradients and stronger longitudinal short-range wakefield. As shown in Figs.3(middle) and 5(bottom-left) and summarized in Table 2, the chirp and the rms relative projective energy spread of the C-band linac are almost same as those of S-band linac though the RF phase of C-band linac is 10 degree for 30 MV/m. In addition, the C-band linac can supply a good linearity in the longitudinal phase space, a low sensitivity of the RF phase error due to the near on-crest RF phase operation and more modulators, a low sensitivity of misalignment of linac structures due to

a low transverse short-range wakefield for a short bunch length and due to a short linac length, a narrow FEL photon beam bandwidth due to a small projected energy spread of 0.014%, and a short linac length and a compact XFEL facility [3].

However, the X-band linac supplies a higher nonlinearity in the longitudinal phase space due to a higher longitudinal short-range wakefield, a higher RF jitter sensitivity due to a higher SLED gain and more linac structures per modulator, and smaller number of modulators. a higher sensitivity of misalignment of linac structures due to a higher transverse short-range wakefield, a more wide FEL photon beam bandwidth due to a bigger projected energy spread of 0.024% [3].

## SUMMARY & ACKNOWLEDGMENTS

Although the X-band linac technology can supply a compact XFEL facility, its performance is worse than the C-band RF linac based XFEL facility due to many reasons as described in previous section. The X-band linac can supply a higher gradient to make a more compact XFEL facility. However, in this case, we may feel difficulty to control the energy chirp, the nonlinearity in the longitudinal phase space, and to get a small projected energy spread and a small XFEL photon beam bandwidth, and to reduce RF jitter sensitivity. In case of the S-band linac technology, there is also a limitation to build a compact XFEL facility due to its weak longitudinal short-range wakefield. But the C-band RF linac technology can supply proper short-range wakefields and various other advantages for a compact XFEL facility.

Y. Kim gives sincere thanks to Prof. T. Shintake and Dr. T. Inagaki of RIKEN/SPring-8, Prof. K. Yokoya and Prof. H. Matsumoto of KEK, Mr. S. Miura of MHI, Mr. O. Yushiro of Toshiba, Dr. H. Braun, Dr. M. Pedrozzi, Dr. S. Reiche, Dr. T. Garvey, Dr. J.-Y. Raguin, and Dr. M. Dehler of PSI, Dr. Y. Sun, Dr. C. Adolphsen, Dr. J. Wu, Dr. Z. Huang, and Prof. T. Raubenheimer of SLAC, Dr. P. Emma of LBNL, Prof. W. Namkung, Prof. M. H. Cho, and Prof. I. S. Ko of PAL/POSTECH, Dr. K. Floettmann of DESY, Dr. M. Borland and Prof. K.-J. Kim of APS, Prof. S. Y. Lee of Indiana University, Dr. B. Carlsten of LANL, and Dr. A. Hutton and Dr. H. Areti of Jefferson Lab for their valuable discussions and encouragements on this work.

## REFERENCES

- [1] T. Ishikawa *et al.*, Nature Photonics **6**, 540 (2012).
- [2] <http://www.psi.ch/swissfel/swissfel>
- [3] Y. Kim, <http://www.physics.isu.edu/~yjkim/talks/fls2012.pdf>
- [4] T. O. Raubenheimer, Phys. Rev. ST Accel. Beams **3**, 121002 (2000).
- [5] K. Bane, SLAC Report, SLAC-PUB-11829, 2006.